

## VIBRATIONAL SPECTROSCOPIC AND QUANTUM CHEMICAL STUDY OF ANTIMONY(III) OXIDE

E. I. Voit, A. E. Panasenko, and L. A. Zemnukhova

UDC 535.375:546.863.31

IR and Raman spectroscopy are used to study cubic and orthorhombic modifications of  $\text{Sb}_2\text{O}_3$ . Vibrational spectra are calculated in the approximation of density functional theory; the bands are assigned. Based on the assignment made, vibrational spectra of the  $\alpha\text{-Sb}_3\text{O}_2\text{F}_5$  compound are analyzed.

**Keywords:** antimony(III) oxide, DFT, IR, Raman, vibrational spectroscopy.

### INTRODUCTION

Antimony(III) oxide is presently used as a stable white pigment to produce paints, polymers, rubber ware, glasses, and enamels, as UV-filter to increase thermal and fire resistance, light scattering of materials, and to increase their conductivity, and it is also applied to manufacture catalysts, sorbents, and medical drugs [1-4]. In a number of cases, the possibility to use  $\text{Sb}_2\text{O}_3$  is determined by the structure of the compound. There are two crystalline modifications of antimony(III) oxide: low temperature cubic  $\alpha$ -modification senarmontite and high temperature orthorhombic  $\beta$ -modification valentinite [5, 6]. It is differences in their structure that are responsible for different physicochemical properties.

At present, several methods are known to synthesize  $\text{Sb}_2\text{O}_3$  oxide [7-9] that involve hydrolysis of different antimony(III) compounds, the phase composition of the product being dependent on synthesis conditions. Still, regularities of the formation of cubic or orthorhombic forms of antimony(III) oxide during hydrolysis have been insufficiently studied. Antimony(III) oxide currently produced industrially is almost not controlled by the phase composition.

Vibrational spectroscopy that provides structural information is often used to control the composition and quality of synthesized antimony(III) compounds along with other physicochemical methods of analysis. A detailed analysis of vibrational spectra is absent for the majority of oxygen-containing antimony(III) compounds, including  $\text{Sb}_2\text{O}_3$ , except some attempts to assign bands in the spectrum [10-14]. This work presents a theoretical calculation of vibrational spectra of antimony(III) oxide; the bands are assigned and compared with experimental IR and Raman spectra. Vibrational spectra of antimony(III) oxofluoride  $\text{Sb}_3\text{O}_2\text{F}_5$  are analyzed.

### EXPERIMENTAL

In order to measure vibrational spectra we used the cubic modification of antimony(III) oxide produced by Merck (chemically pure) and the orthorhombic modification of  $\text{Sb}_2\text{O}_3$  that we prepared by hydrolysis of antimony(III) chloride (purity grade) in boric acid solution.

Antimony(III) oxofluoride was obtained by hydrolysis of antimony(III) fluoride (reagent grade) in acetic acid solution. The synthesis product was identified as  $\alpha\text{-Sb}_3\text{O}_2\text{F}_5$  by methods of chemical and X-ray phase analysis [15].

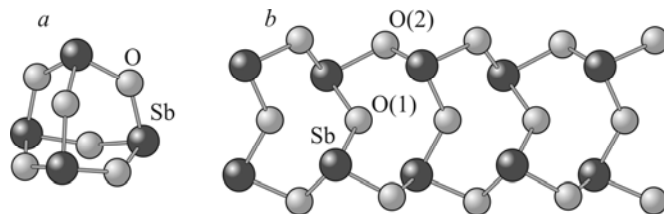


**Fig. 1.** Model clusters:  $[\text{Sb}_4\text{O}_6]$  for  $\alpha\text{-Sb}_2\text{O}_3$  (a) and  $[\text{Sb}_{10}\text{O}_{15}]$  for  $\beta\text{-Sb}_2\text{O}_3$  (b).

IR spectra of samples in the region of  $250\text{ cm}^{-1}$  to  $4000\text{ cm}^{-1}$  were measured in vaseline oil at ambient temperature using a Shimadzu FTIR Prestige-21 spectrometer with a resolution of  $2\text{ cm}^{-1}$ . The low frequency region of spectra up to  $150\text{ cm}^{-1}$  was recorded on a Vertex 70 spectrophotometer. Raman spectra of  $\alpha\text{-Sb}_2\text{O}_3$  and  $\alpha\text{-Sb}_3\text{O}_2\text{F}_5$  were obtained with a resolution of  $2\text{ cm}^{-1}$  on a RFS100/S spectrometer in backscattering mode (Nd laser: YAG,  $\lambda = 1064\text{ nm}$ , 100 mW). The Raman spectrum of  $\beta\text{-Sb}_2\text{O}_3$  was recorded using a TRiVista spectrometer with a scattering angle of  $90^\circ$  (Ar laser: Spectra Physics,  $\lambda = 488\text{ nm}$ ).

Quantum chemical simulation of cubic and orthorhombic modifications of antimony(III) oxide was performed using the GAMESS package [16] at the density functional theory level with the B3LYP exchange-correlation potential. We used the SBKJC valence basis set [17] as the basis set for all atoms in combination with a quasi-relativistic core potential supplemented by the  $d$ -diffusion function for oxygen atoms. All calculations were performed on a 16-processor Linux-cluster in Institute of Chemistry, Far East Division, Russian Academy of Sciences.

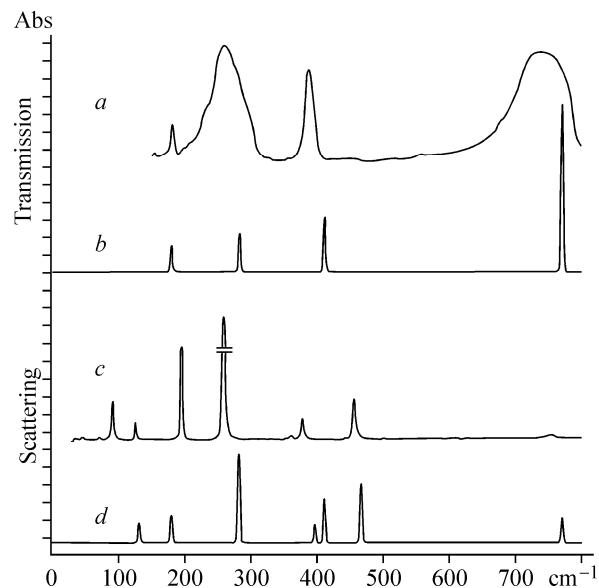
## RESULTS AND DISCUSSION

Structures of cubic and orthorhombic modifications of antimony(III) oxide were studied by X-ray diffraction analysis [5, 6]. The structure of the cubic modification is described by  $\text{Sb}_4\text{O}_6$  molecular units in which all oxygen atoms occupy bridging positions and are in the vertices of the octahedron, whereas antimony atoms lie to the outside of its four faces. In the orthorhombic modification, the structure is made of infinite double chains formed by coordination tetrahedra bridged by oxygen atoms. Fig. 1 depicts model clusters for two modifications used in calculations.

Vibrational spectra of  $\alpha\text{-Sb}_2\text{O}_3$  were calculated using the  $[\text{Sb}_4\text{O}_6]$  cluster with  $T_d$  symmetry (Fig. 1a) that is the main fragment in the crystal structure of the compound under study [6]. Full optimization of geometric parameters was performed. The calculated optimal Sb–O distance is  $1.953\text{ \AA}$  ( $1.977\text{ \AA}$ , according to X-ray diffraction data). Fig. 2 and Table 1 present experimental and calculated IR and Raman spectra of  $\alpha\text{-Sb}_2\text{O}_3$ . Good agreement is observed between experimental and calculated data.

High tetrahedral symmetry of the selected cluster results in a small number of bands in vibrational spectra. An intense band at  $741\text{ cm}^{-1}$  in the IR spectrum (at  $765\text{ cm}^{-1}$  in theoretical) is responsible for symmetric combinations of stretching vibrations  $\nu_{\text{asym}}$  (SbO). Below  $460\text{-}360\text{ cm}^{-1}$ , the bands lie that correspond to vibrations caused by the deformation of Sb–O–Sb bonds. These vibrations are directed to the symmetry center of the tetrahedral cluster and can be also considered stretching  $\nu_{\text{sym}}$  (SbO) because they lead to a considerable ( $0.09\text{-}0.03\text{ \AA}$ ) change in the Sb–O distance. In the IR spectrum, the most intense deformation band at  $260\text{ cm}^{-1}$  (at  $280\text{ cm}^{-1}$  in theoretical) has  $A_1$  symmetry. Combinations of wagging and twisting deformation vibrations lie below (Table 1).

Vibrational spectra of  $\beta\text{-Sb}_2\text{O}_3$  were calculated using the  $[\text{Sb}_{10}\text{O}_{15}]$  cluster with  $C_2$  symmetry (Fig. 1b) that is the basic fragment in the structure of this compound [5]. Full optimization of the geometric parameters of the cluster did not yield reliable geometry because of diverse possible stable configurations in the structure of antimony oxides [18]. When atoms were fixed at the chain boundaries (Fig. 1b), the calculated optimal Sb–O(2) distances slightly differed from crystallographic data ( $1.89\text{ \AA}$ ,  $2.11\text{ \AA}$ ), while the Sb–O(1) distances were largely overestimated ( $2.15\text{ \AA}$ ). Therefore the

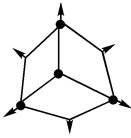
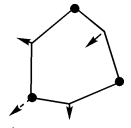
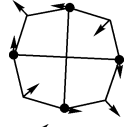
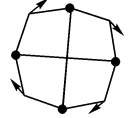


**Fig. 2.** Experimental ((a) IR, (c) Raman) spectra of  $\alpha$ - $\text{Sb}_2\text{O}_3$ ; theoretical ((b) IR, (d) Raman) spectra of the  $[\text{Sb}_4\text{O}_6]$  cluster ( $T_d$ ).

**TABLE 1.** Experimental IR and Raman Spectra of  $\alpha$ - $\text{Sb}_2\text{O}_3$  and Calculated Frequencies for the  $[\text{Sb}_4\text{O}_6]$  Cluster ( $T_d$ ) with Band Assignment

Experiment		DFT/B3LYP/SBKJ+d				Assignment	$\nu$ , $\text{cm}^{-1}$ [10-14]	
$\nu$ , $\text{cm}^{-1}$		$\nu$ , $\text{cm}^{-1}$	Symmetry	Intensity*				
IR	Raman			IR	Raman			
1	2	3	4	5	6	7	8	
741	—	765	$T_2$	11.9	1.7	$\nu_{\text{sym}}(\text{SbO}_3)$ sym comb $\nu_{\text{asym}}$ ( $\text{Sb} \rightarrow \text{O} \rightarrow \text{Sb}$ )		740-717
537	—	574	$T_1$	0.0	0.0	$\nu_{\text{asym}}(\text{SbO}_3)$ asym comb $\nu_{\text{asym}}$ ( $\text{Sb} \rightarrow \text{O} \rightarrow \text{Sb}$ )		590-550
460	460	465	$A_1$	0	90.0	$\nu_{\text{sym}}(\text{SbO}_3)$ sym comb $\nu_{\text{sym}}$ ( $\text{Sb} \rightarrow \text{O} \leftarrow \text{Sb}$ )		458-452
385	383	409	$T_2$	1.5	6.2	$\nu_{\text{sym}}(\text{SbO}_3)$ asym comb $\nu_{\text{sym}}$ ( $\text{Sb} \rightarrow \text{O} \leftarrow \text{Sb}$ )		381-375
—	367	394	$E$	0	2.0	$\nu_{\text{asym}}(\text{SbO}_3)$ sym comb $\nu_{\text{sym}}$ ( $\text{Sb} \rightarrow \text{O} \leftarrow \text{Sb}$ )		364-359
280	—	282	$T_2$	0.6	0.1	$\delta_{\text{sym}}(\text{SbO}_2)$ sym comb $\delta_{\text{sym}}$ ( $\text{Sb} \rightarrow \text{O} \leftarrow \text{Sb}$ )		—

TABLE 1. (Continued)

1	2	3	4	5	6	7	8	
260	263	280	$A_1$	0	254.0	$\delta_{\text{sym}}(\text{SbO}_3)$ sym comb $\delta_{\text{sym}}$ ( $\text{O} \rightarrow \text{Sb} \leftarrow \text{O}$ )		261-256
179	198	179	$T_2$	0.4	2.8	$\delta_{\text{asym}}(\text{SbO}_3)$ asym comb $\delta_{\text{sym}}$ ( $\text{Sb} \rightarrow \text{O} \leftarrow \text{Sb}$ )		197-192
—	127	126	$E$	0	2.4	$\delta_{\text{asym}}(\text{SbO}_3)$ sym comb $\delta_{\text{sym}}$ ( $\text{Sb} \rightarrow \text{O} \leftarrow \text{Sb}$ )		124-121
—	92	109	$T_1$	0	0.0	$\delta_{\text{asym}}(\text{SbO}_2)$ asym comb $\delta_{\text{asym}}$ ( $\text{Sb} \rightarrow \text{O} \leftarrow \text{Sb}$ )		87-84

\*Intensity of the calculated bands is measured in  $\text{D}^2/\mu\text{A}^2$  in IR spectra and in  $\text{A}^4/\mu$  in Raman spectra.

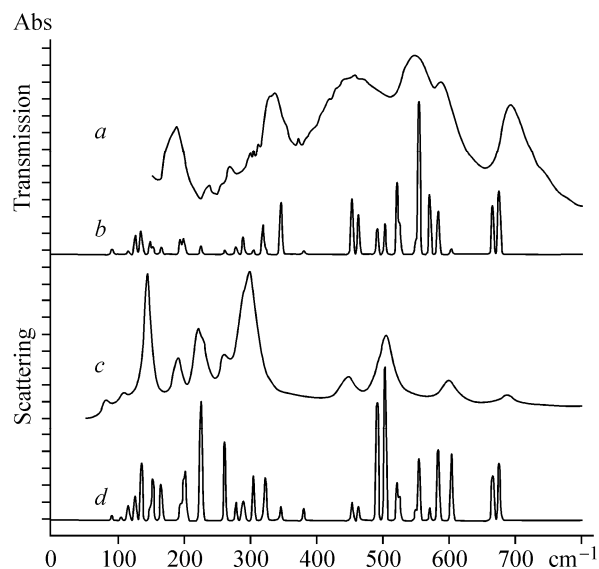


Fig. 3. Experimental ((a) IR, (c) Raman) spectra of  $\beta\text{-Sb}_2\text{O}_3$ ; theoretical ((b) IR, (d) Raman) spectra of the  $[\text{Sb}_{10}\text{O}_{15}]$  cluster ( $C_2$ ).

vibrational spectrum was calculated using the crystallographic geometric parameters (Sb–O(1) distance was 2.024 Å; Sb–O(2): 1.984 Å and 2.024 Å) and with fixed atoms at the chain boundaries. In the calculated spectra, one imaginary frequency at  $47\text{ cm}^{-1}$  is found that is due to lattice vibrations which coincide in direction with chain bending. Table 2 presents the calculated frequencies and the assignment of bands performed in IR and Raman spectra.

Different boundary conditions of chain links resulted in an increase in the number of frequencies corresponding to similar parts. Groups of similar vibrations are marked out in Table 2. Fig. 3 shows experimental and calculated spectra of  $\beta\text{-Sb}_2\text{O}_3$ .

According to calculations, the region of  $750\text{ cm}^{-1}$  to  $300\text{ cm}^{-1}$  can be conventionally considered the region of stretching vibrations occurring in the chain plane (Fig. 1b) and leading to a substantial change in the Sb–O distance. Below  $300\text{ cm}^{-1}$ , the deformation vibrations of Sb–O bonds lie, directed at an angle to the chain plane (Fig. 1b).

An intense wide band at  $741\text{ cm}^{-1}$  in the experimental IR spectrum of  $\alpha\text{-Sb}_2\text{O}_3$  (Fig. 2a) splits into two doublets (Fig. 3a) at  $720\text{ cm}^{-1}$  (shoulder),  $688\text{ cm}^{-1}$  and  $589\text{ cm}^{-1}$ ,  $540\text{ cm}^{-1}$  in the spectrum of  $\beta\text{-Sb}_2\text{O}_3$  which correspond to symmetric and antisymmetric combinations of  $\nu_{\text{asym}}$ . The vibrations involving a certain type of bridging O(1) and O(2) oxygen atoms correspond to each of the doublets (Fig. 1, Table 2).

In the experimental IR spectrum of  $\alpha\text{-Sb}_2\text{O}_3$ , the second intense narrow band at  $385\text{ cm}^{-1}$  ( $T_2$ ) is responsible for antisymmetric combinations of stretching vibrations  $\nu_{\text{sym}}(\text{SbOSb})$ ; in the Raman spectrum, bands in the region of  $460\text{ cm}^{-1}$  ( $A_1$ ) and  $367\text{ cm}^{-1}$  ( $E$ ) correspond to these vibrations. In the IR spectrum of the orthorhombic form of antimony(III) oxide, two bands are already seen:  $500\text{-}400\text{ cm}^{-1}$  (wide) and  $333\text{-}326\text{ cm}^{-1}$ , corresponding to symmetric and antisymmetric combinations of stretching  $\nu_{\text{sym}}$  involving O(1) and O(2) respectively. As shown by calculations, a moderately intense band at  $960\text{ cm}^{-1}$  in the IR spectrum of  $\alpha\text{-Sb}_2\text{O}_3$ , mentioned in [14], does not relate to the ideal structure of this compound. According to our data, the band at  $960\text{ cm}^{-1}$  is not seen in the spectrum of the cubic modification of antimony(III) oxide measured on KRr glass.

**TABLE 2.** Experimental Frequencies in Vibrational Spectra of  $\beta\text{-Sb}_2\text{O}_3$  and Calculated Normal Frequencies of the  $[\text{Sb}_{10}\text{O}_{15}]$  Cluster ( $C_2$ ) and their Assignment

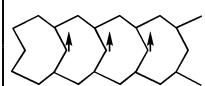
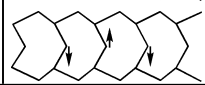
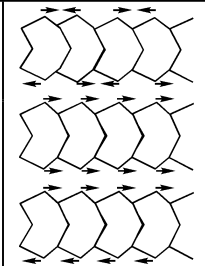
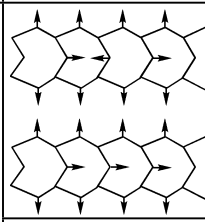
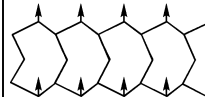
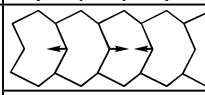
Experiment		DFT/B3LYP/SBKJC+d				Assignment	v, $\text{cm}^{-1}$ [10-14]		
IR	Raman	v, $\text{cm}^{-1}$	Symmetry	Intensity			IR	Raman	
1	2	3	4	5	6	7	8	9	
720		672	<i>B</i>	2.2	5041	sym and asym comb $\nu_{\text{asym}}(\text{Sb}\rightarrow\text{O}(1)\rightarrow\text{Sb})$		740	
688	686	663	<i>B</i>	1.2	2905			—	690
589	598	600	<i>A</i>	0.0	6668	sym and asym comb $\nu_{\text{asym}}(\text{Sb}\rightarrow\text{O}(2)\rightarrow\text{Sb})$		585	602
		581	<i>A</i>	0.9	24,300				
		552	<i>A</i>	10.4	14,776				
540	—	567	<i>B</i>	1.7	248			540	—
		547	<i>B</i>	0.1	188				
		523	<i>B</i>	0.4	711				
		501	<i>B</i>	2.7	2140				
482	504	519	<i>A</i>	0.4	115,039	sym and asym comb $\nu_{\text{sym}}(\text{Sb}\rightarrow\text{O}(2)\leftarrow\text{Sb})$		488	502
		501	<i>A</i>	2.7	2140				
		489	<i>A</i>	0.1	23,870				
457	447	460	<i>B</i>	0.7	250			455	449
428		450	<i>B</i>	1.4	405				
—	—	379	<i>B</i>	0.0	248	sym and asym comb $\nu_{\text{sym}}(\text{Sb}\rightarrow\text{O}(1)\leftarrow\text{Sb})$		—	—
333	—	344	<i>A</i>	1.2	250				—
326		311	<i>A</i>	0.51					

TABLE 2. (Continued)

1	2	3	4	5	6	7		8	9
—	299	316 302 288	<i>B</i> <i>B</i> <i>B</i>	0.33 0.01 0.04	40 1534 256	sym and asym comb $\delta\text{SbO}_2$ $\delta(\text{O}(2) \text{ Sb O}(1))$ $\text{Sb-O}(2) = (1.894)$	Scissoring	—	294
—	263	286 276 259	<i>A</i> <i>A</i> <i>A</i>	0.07 0.03 0.00	208 541 7617			269	
—	221	223 211	<i>A</i> <i>B</i>	0.04 0.07	21,691 36	sym and asym comb $\delta\text{SbO}_2$ $\delta(\text{O}(2) \text{ Sb O}(2))$ $\text{Sb-O}(2) = (1.894,$ $2.024)$	Wagging	—	223
188	190	201 200 197 192	<i>B</i> <i>A</i> <i>B</i> <i>B</i>	0.00 0.01 0.25 0.11	65 2051 201 411			Twisting	—
—	145 110 82	163 151 146 135 133 124 114 89 84	<i>A</i> <i>A</i> <i>B</i> <i>A</i> <i>B</i> <i>A</i> <i>B</i> <i>B</i> <i>A</i>	0.21 0.17 0.20 0.02 0.05 0.52 0.02 0.02 0.04	1800 2842 234 92 4681 300 50 43 12,469	sym and asym comb $(\text{SbO}_3\text{-SbO}_3)$	Lattice vibrations	—	140 103 71

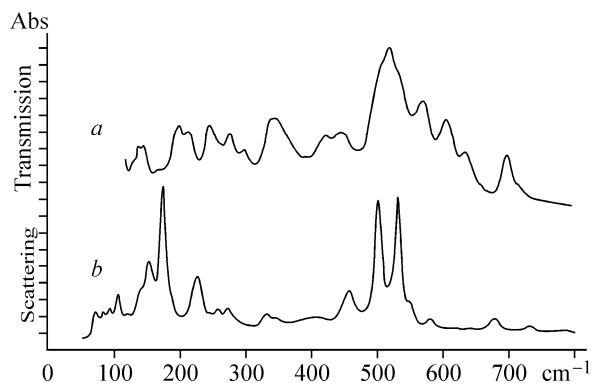


Fig. 4. Experimental IR (a), Raman (b) spectra of antimony(III) oxofluoride  $\text{Sb}_3\text{O}_2\text{F}_5$ .

The region of deformation vibrations in the experimental IR spectrum of  $\alpha\text{-Sb}_2\text{O}_3$  starts with a wide band with a maximum at  $260 \text{ cm}^{-1}$ . In the Raman spectrum of  $\alpha\text{-Sb}_2\text{O}_3$ , this band has the highest intensity and corresponds to the totally symmetric vibration of  $A_1$  symmetry. In the IR spectrum, according to calculations, its shoulder conceals the  $\delta_{\text{sym}}(\text{SbOSb})$  band ( $280 \text{ cm}^{-1}$ ) corresponding to vibrations perpendicular to the Sb–O bond direction. In the spectrum of  $\beta\text{-Sb}_2\text{O}_3$ , the bending region starts with a wide band near  $\sim 300 \text{ cm}^{-1}$ . The majority of deformation bands of  $\beta\text{-Sb}_2\text{O}_3$  have a considerable half-width and the intensity smaller than that of  $\alpha\text{-Sb}_2\text{O}_3$  due to lower symmetry of the lattice ( $C_2$ ). Lattice vibrations lie below  $165 \text{ cm}^{-1}$  in the spectrum of  $\beta\text{-Sb}_2\text{O}_3$ , and here  $[\text{SbO}_3]^{3-}$  groups vibrate without changing bond lengths and OSbO internal angles. When the lattice vibrates,  $[\text{SbO}_3]^{3-}$  groups move jointly in three directions, and only SbOSb external angles change.

Fig. 4 depicts IR and Raman spectra of the  $\alpha$ -modification of antimony(III) oxofluoride  $\text{Sb}_3\text{O}_2\text{F}_5$ . Its structure consists of four types of antimony polyhedra:  $\text{Sb}(1)\text{F}_4\text{E}$ ,  $\text{Sb}(2)\text{F}_3\text{OE}$ ,  $\text{Sb}(3)\text{O}_4\text{E}$ , and  $\text{Sb}(4)\text{O}_4\text{E}$  (E is the lone electron pair) [15]. It is seen from the vibrational spectra of  $\alpha$ - $\text{Sb}_3\text{O}_2\text{F}_5$  and the above assignment of frequencies for  $\text{Sb}_2\text{O}_3$  that all oxygen atoms in the oxofluoride structure are bridging because the band at  $700\text{ cm}^{-1}$  in the IR spectrum coincides in form and position with that for  $\beta$ - $\text{Sb}_2\text{O}_3$ . The occurrence of additional intense bands in the  $630$ - $520\text{ cm}^{-1}$  region indicates the presence of a large number of terminal fluorine atoms [19, 20]. The presence of the most noticeable band at  $220\text{ cm}^{-1}$  in the Raman spectrum corresponds to symmetric angular deformations of a more coordinately saturated polyhedron than that in the structure of oxides. Amplification of bands in the bending region of the IR spectrum indicates a reduction of the full lattice symmetry in comparison with the valentinite lattice and a more complicated general motif of the structure, which is consistent with X-ray diffraction data.

## CONCLUSIONS

Based on quantum chemical calculations, the bands are assigned in the experimental spectra of cubic and orthorhombic modifications of antimony(III) oxide. The analysis of vibrational spectra makes it possible to unambiguously distinguish phases of  $\text{Sb}_2\text{O}_3$  and to plan and control the synthesis of oxygen-containing compounds of antimony(III) with particular structural properties. The results of this work enable the identification of some bands in spectra of oxygen-containing compounds of antimony(III) and the assumptions about their structure.

## REFERENCES

1. B. Pillep and P. Behrens, *J. Phys. Chem. B*, **103**, No. 44, 9595-9603 (1999).
2. C. Ye, G. Meng, L. Zhang, et al., *Chem. Phys. Lett.*, **363**, 34-38 (2002).
3. Y. Zhang, G. Li, J. Zhang, et al., *Nanotechnology*, **15**, 762-765 (2004).
4. J. Tan, L. Shen, X. Fu, et al., *Dyes and Pigments*, **61**, 31-38 (2004).
5. Ch. Svensson, *Acta Crystallogr.*, **B30**, 458-461 (1974).
6. Ch. Svensson, *ibid.*, **B31**, 2016-2018 (1975).
7. I. L. Knunyants (ed.), in: *Chemical Encyclopedia* [in Russian], Sov. Éntsikl., Moscow (1983).
8. Yu. V. Karyakin and I. I. Angelov, *Pure Chemical Compounds* [in Russian], Khimiya, Moscow (1974).
9. L. Guo, Z. Wu, T. Liu, et al., *Chem. Phys. Lett.*, No. 318, 49-52 (2000).
10. J. R. Ferraro, *Low-Frequency Vibrations of Inorganic and Coordination Compounds*, Plenum Press, New York (1971).
11. M. O. Guerrero-Perrez, J. L. G. Fierro, M. A. Vicente, et al., *J. Catal.*, **206**, 339-348 (2002).
12. P. J. Miller and A. Charles, *Spectrochim. Acta Part A: Molecular Spectroscopy*, **38**, No. 5, 555-559 (1982).
13. M. A. Banãres, M. O. Guerrero-Perez, J. L. G. Fierro, et al., *J. Mater. Chem.*, **12**, 3337-3342 (2002).
14. C. A. Cody, L. DiCarlo, and R. K. Darlington, *Inorg. Chem.*, **18**, No. 6, 1572-1576 (1979).
15. A. A. Udovenko, L. A. Zemnukhova, E. V. Kovaleva, and G. A. Fedorishcheva, *Koordinats. Khim.*, **30**, No. 8, 1-8 (2004).
16. M. W. Schmidt, K. K. Baldridge, J. A. Boatz, et al., *J. Comput. Chem.*, **14**, 1347-1363 (1993).
17. W. J. Stevens, H. Basch, M. Krauss, et al., *Can. J. Chem.*, **70**, 612-630 (1992).
18. B. Kaiser, T. M. Bernhardt, M. Kinne, et al., *J. Chem. Phys.*, **110**, No. 3, 1437-1449 (1999).
19. N. M. Laptash, E. V. Kovaleva, A. A. Mashkovskii, et al., *J. Struct. Chem.*, **48**, No. 5, 848-854 (2007).
20. R. L. Davidovich, T. A. Kaidalova, T. F. Levchishina, and V.I. Sergienko, *Atlas of Infrared Spectra and X-ray Data for Complex Fluorides of Metals of Groups IV and V* [in Russian], Nauka, Moscow (1972).